D1-82-0147

BOEING SCIENTIFIC RESEARCH LABORATORIES

Interaction of a Plane Jet with a Magnetic Field

F. D. Hains

December 1961

D1-82-0147

BOEING SCIENTIFIC RESEARCH LABORATORIES

FLIGHT SCIENCES LABORATORY REPORT NO. 55

INTERACTION OF A PLANE JET WITH A MAGNETIC FIELD

by

F. D. Hains

December 1961

INTERACTION OF A PLANE JET WITH A MAGNETIC FIELD

by F. D. Hains

Boeing Scientific Research Laboratories

ABSTRACT

An analysis is made of the distortion of a plane, supersonic free jet by a strong magnetic field. The field is created by a straight wire placed outside of the jet and normal to the plane of flow. The entire flow field is obtained numerically by the method of characteristics for several locations of the wire when the magnetic Reynolds number is small. The magnetic field tends to decelerate the flow to sonic velocity without the formation of shocks. The resultant force acting on the wire is found to vary linearly with the interaction parameter N for values of N as large as 0.1.

I. INTRODUCTION

A partially ionized gas issues from an orifice with supersonic velocity and atmospheric pressure. It forms a two-dimensional, free jet which would continue unimpeded if it did not encounter a magnetic field since viscous and heat transfer effects are neglected. This report considers the interaction of such an ionized jet with a powerful magnetic field.

Two cases are studied which differ only in the location of the wire producing the magnetic field. In the first case, shown in Figure 1, the wire is placed far downstream of the jet exit so that the boundary conditions of uniform flow at the exit are still valid. In the second case, the line has been moved to the plane of the exit of the jet as shown in Figure 2. Although the magnetic field enters the nozzle, the same boundary conditions are used so that comparison can be made of the effect of the location of the wire. It can be assumed for this case that the gas becomes conducting just at the exit of the nozzle.

In order to uncouple Maxwell's equations from the fluid mechanics equations, the magnetic Reynolds number R_m is assumed small. The interaction parameter N is assumed to be of first order, requiring numerical solution of the resultant non-linear equations by the method of characteristics. Results of a further simplification by linearization for small N are presented in Reference 1.

II. DERIVATION OF THE STEADY FLOW EQUATIONS

The steady flow of a partially ionized gas in the presence of a magnetic field is described by the following continuum relations:

Momentum

$$\tilde{\rho}(\vec{q} \cdot \vec{\nabla})\vec{q} + \vec{\nabla}\tilde{p} = \vec{j} \times \vec{B} \tag{1}$$

Continuity

$$\vec{\nabla} \cdot \tilde{\rho}\vec{q} = 0 \tag{2}$$

Energy

$$\vec{q} \cdot \vec{\nabla}\left(\tilde{i} + \frac{\tilde{q}^2}{2}\right) = \vec{q} \cdot (\vec{j} \times \vec{B}) + \frac{\vec{j} \cdot \vec{j}}{\tilde{\sigma}} \tag{3}$$

Ohm's Law

$$\vec{j} = \vec{\sigma}(\vec{E} + \vec{q} \times \vec{B}) \tag{4}$$

Maxwell's Equations

$$\vec{\nabla} \times \vec{B} = \tilde{\mu}\vec{j} \tag{5}$$

$$\vec{\nabla} \times \vec{E} = 0 \tag{6}$$

$$\vec{\nabla} \cdot \vec{B} = 0 \tag{7}$$

First and Second Laws of Thermodynamics

$$\tilde{T}\vec{\nabla}\tilde{s} = \vec{\nabla}\tilde{i} - \frac{\vec{\nabla}\tilde{p}}{\tilde{\rho}} \tag{8}$$

Gas Law

$$\tilde{p} = \tilde{\rho}R\tilde{T} \tag{9}$$

Vector quantities are indicated by an arrow. These include the velocity $\vec{q}$, the current $\vec{j}$, the electric field $\vec{E}$, and the magnetic field $\vec{B}$. Scalar quantities in their dimensional form are indicated by a tilda. These include pressure $\tilde{p}$, density $\tilde{\rho}$, temperature $\tilde{T}$, enthalpy $\tilde{i}$, entropy $\tilde{S}$, electrical conductivity $\tilde{\sigma}$, and permeability $\tilde{\mu}$.

The inclusion of magnetogasdynamic effects has added new equations as well as additional terms to the existing gas dynamic equations. The magnetic body force term has been added to the right hand side of the momentum equation, and the right hand side of the energy equation contains two additional terms which represent the work done by the magnetic body force and Joule heating. The effects of heat transfer and viscous dissipation have been neglected. For the two-dimensional jet the electric field must vanish.

$$\vec{E} = 0 \tag{10}$$

Making use of this fact to simplify Ohm's Law, the energy equation (3) reduces to

$$\vec{q} \cdot \vec{\nabla}\left(\tilde{i} + \frac{\tilde{q}^2}{2}\right) = 0 \tag{11}$$

which states the total enthalpy $\tilde{H}$ must be conserved. Thus, the work done by the magnetic body force just balances the Joule heating so that the flow remains isoenergetic. The more general case where $\vec{E}$ does not vanish could still be solved by the method of characteristics, but the choice of dependent variables would be different

since the total enthalpy would have to be calculated for each point on the characteristic net.

Making use of the vector identity

$$(\vec{q} \cdot \vec{\nabla})\vec{q} \equiv \vec{\nabla} \frac{\tilde{q}^2}{2} - \vec{q} \times (\vec{\nabla} \times \vec{q}) \tag{12}$$

the pressure can be eliminated between Eqs. (1) and (8) leading to

$$\vec{\nabla}\tilde{H} - \vec{q} \times (\vec{\nabla} \times \vec{q}) - \tilde{T}\vec{\nabla}\tilde{S} = \frac{\tilde{\sigma}}{\tilde{\rho}} (\vec{q} \times \vec{B}) \times \vec{B} \tag{13}$$

Scalar multiplication of this equation by $\vec{q}$ results in

$$\tilde{q} \cdot \vec{\nabla}\tilde{S} = \frac{\tilde{\sigma}}{\tilde{\rho}\tilde{T}} (\vec{q} \times \vec{B})^2 \tag{14}$$

In scaler form, this is

$$\tilde{u} \frac{\partial \tilde{S}}{\partial \tilde{x}} + \tilde{v} \frac{\partial \tilde{S}}{\partial \tilde{y}} = \frac{\tilde{\sigma}}{\rho T} \left(\tilde{u}\tilde{B}_y - \tilde{v}\tilde{B}_x \right)^2 \tag{15}$$

From these relations it is clear that the flow will be rotational and entropy will increase along streamlines.

Using Eqs. (8) and (9), the pressure can be expressed in terms of the other variables.

$$\left.\begin{aligned} \frac{\partial \tilde{p}}{\partial \tilde{x}} &= \frac{\tilde{\rho}\tilde{a}^2}{\gamma} \frac{\partial \tilde{S}}{\partial \tilde{x}} + \tilde{a}^2 \frac{\partial \tilde{\rho}}{\partial \tilde{x}} \\ \frac{\partial \tilde{p}}{\partial \tilde{y}} &= \frac{\tilde{\rho}\tilde{a}^2}{\gamma} \frac{\partial \tilde{S}}{\partial \tilde{y}} + \tilde{a}^2 \frac{\partial \tilde{\rho}}{\partial \tilde{y}} \end{aligned}\right\} \tag{16}$$

The final form of the momentum Eq. (1) is obtained by elimination of the pressure with Eq. (16) and the current with Eq. (4).

$$\tilde{\rho}\tilde{u}\frac{\partial\tilde{u}}{\partial\tilde{x}} + \tilde{\rho}\tilde{v}\frac{\partial\tilde{u}}{\partial\tilde{y}} + \frac{\tilde{\rho}\tilde{a}^2}{\gamma}\frac{\partial\tilde{S}}{\partial\tilde{x}} + \tilde{a}^2\frac{\partial\tilde{\rho}}{\partial\tilde{x}} = -\tilde{\sigma}\tilde{B}_y\left(\tilde{u}\tilde{B}_y - \tilde{v}\tilde{B}_x\right) \qquad (17)$$

$$\tilde{\rho}\tilde{u}\frac{\partial\tilde{v}}{\partial\tilde{x}} + \tilde{\rho}\tilde{v}\frac{\partial\tilde{v}}{\partial\tilde{y}} + \frac{\tilde{\rho}\tilde{a}^2}{\gamma}\frac{\partial\tilde{S}}{\partial\tilde{y}} + \tilde{a}^2\frac{\partial\tilde{\rho}}{\partial\tilde{y}} = \tilde{\sigma}\tilde{B}_x\left(\tilde{u}\tilde{B}_y - \tilde{v}\tilde{B}_x\right) \qquad (18)$$

The scaler form of the continuity equation is

$$\frac{\partial(\tilde{\rho}\tilde{u})}{\partial\tilde{x}} + \frac{\partial(\tilde{\rho}\tilde{v})}{\partial\tilde{y}} = 0 \qquad (19)$$

At this point it is convenient to non-dimensionalize by introducing the new variables

$$\left.\begin{aligned} u &= \tilde{u}/u_\infty \quad & v &= \tilde{v}/u_\infty \quad & x &= \tilde{x}/L \quad & T &= \tilde{T}/T_\infty \\ a &= \tilde{a}/a_\infty \quad & \rho &= \tilde{\rho}/\rho_\infty \quad & B &= \tilde{B}/B_o \quad & S &= \tilde{S}/C_v \\ R_m &= \tilde{\sigma}u_\infty LB_o \quad & N &= \frac{\tilde{\sigma}B_o^2 L}{\rho_\infty u_\infty} \end{aligned}\right\} \qquad (20)$$

The governing equations are tabulated on the following page.

$\frac{\partial u}{\partial x}$	$\frac{\partial u}{\partial y}$	$\frac{\partial v}{\partial x}$	$\frac{\partial v}{\partial y}$	$\frac{\partial \rho}{\partial x}$	$\frac{\partial \rho}{\partial y}$	$\frac{\partial S}{\partial x}$	$\frac{\partial S}{\partial y}$		
ρu	ρv	0	0	a^2	0	$\frac{\rho a^2}{\gamma C_v}$	0	$= -NB_y(UB_y - vB_x)$	(21)
0	0	ρu	ρv	0	a^2	0	$\frac{\rho a^2}{\gamma C_v}$	$= NB_x(UB_y - vB_x)$	(22)
ρ	0	0	ρ	u	v	0	0	$= 0$	(23)
0	0	0	0	0	0	u	v	$= \frac{NK}{\rho a^2}(UB_y - vB_x)^2$	(24)
dx	dy	0	0	0	0	0	0	$= du$	(25)
0	0	dx	dy	0	0	0	0	$= dv$	(26)
0	0	0	0	dx	dy	0	0	$= d\rho$	(27)
0	0	0	0	0	0	dx	dy	$= dS$	(28)

In addition,

$$a^2 = 1 + \frac{\gamma-1}{2} M_\infty^2 (1 - u^2 - v^2) \qquad (29)$$

$$K \equiv \gamma(\gamma-1)M_\infty^2 \qquad (30)$$

When the flow is supersonic, the set of equations (21) - (28) is hyperbolic. Since the set of equations is linear in the first derivatives of dependent variables u, v, ρ and S, these derivatives can be treated as unknowns and solved for in the usual fashion. Once the first derivatives have been obtained, higher derivatives can be

calculated and used in a Taylor series development near the initial line to give the solution over a small region. This could presumably be repeated until the solution is obtained over the entire region of interest.

There are, however, exceptional lines called characteristics along which the determinant of the coefficients of the left hand sides of Eqs. (21) - (28) vanishes. In order to have a solution, the derivatives must be discontinuous across the characteristic. The dependent variables must satisfy certain compatibility relations obtained by replacing one of the columns of the determinant by the right hand sides of Eqs. (21) - (28). These relations are used later to obtain the values of the dependent variables over the entire flow field.

The three characteristics for supersonic flow and their corresponding compatibility relations are given below.

Characteristic I (streamline)

$$\frac{dy}{dx} = \frac{v}{u} \tag{31}$$

Compatibility I-a (energy)

$$v \frac{dS}{dy} = \frac{NK}{\rho a^2}(uB_y - vB_x)^2 \tag{32}$$

Compatibility I-b (momentum)

$$N(uB_y - vB_x) + \rho u \frac{du}{dx} + \rho v \frac{dv}{dx} + \frac{a^2}{M_\infty^2} \frac{d\rho}{dx} + \frac{\rho a^2}{\gamma M_\infty^2} \frac{dS}{dx} = 0 \tag{33}$$

Characteristic II (- sign), III (+ sign) Mach lines

$$\frac{dy}{dx} = \frac{-uv \pm \frac{a}{M_\infty}\sqrt{u^2+v^2-\frac{a^2}{M_\infty^2}}}{\left(\frac{a}{M_\infty}\right)^2 - u^2} \tag{34}$$

Compatibility II and III

$$\frac{-N(uB_y - vB_x)}{\rho}\left(B_y\frac{dx}{dy} + B_x\right) + \frac{N(\gamma-1)M_\infty^2\left[uB_y - vB_x\right]^2\left[v\frac{dx}{dy} - u\right]}{\rho a^2} +$$

$$\frac{a^2}{M_\infty^2}\left[\frac{1}{\gamma(\gamma-1)}\frac{dS}{dy} + \frac{M_\infty^2}{a^2}\frac{u\,du}{dy} + \frac{v\,dv}{dy}\right]\frac{u\frac{dx}{dy}+v}{v\frac{dx}{dy}-u} + u\frac{dv}{dy} - v\frac{du}{dy} = 0 \tag{35}$$

A typical characteristic grid is shown in Figure 3. Through each of the points 1, 2, 3, three characteristics intersect. In the figure, the streamlines are dashed and the Mach lines are solid. Construction of a network of such grids over the entire flow field gives the distribution of velocity, density, entropy, and other flow quantities. The details of this are given in a later section.

In addition to the flow variables there is another quantity which is of interest. This is the reaction force on the wire which produces the magnetic field. For each elemental area of the jet acted upon by the magnetic body force, there is an equal and opposite reaction at the wire according to the Biot-Savart Law*. The components of body force per unit area appear on the right hand

---

* Newton's Law does not strictly apply for these magnetic interactions. This point is discussed further in Reference 2.

sides of Eqs. (21) and (22). Integration over the area of the jet followed by a change in sign gives the components of reaction force at the wire as

$$F_x = \int_{JET} NB_y(uB_y - vB_x)dA \tag{36}$$

$$F_y = -\int_{JET} NB_x(uB_y - vB_x)dA \tag{37}$$

The magnetic field is produced by a steady current flowing through a straight wire located at (x_c, y_c). The field lines are concentric circles about the wire, and the field strength varies inversely with the distance from the wire. The components of this field, non-dimensionalized with respect to the field strength at $(x_c, 2)$ are

$$B_x = \frac{(x - x_c)(y_c - 2)}{(x - x_c)^2 + (y - y_c)^2} \tag{38}$$

$$B_y = \frac{(y_c - y)(y_c - 2)}{(x - x_c)^2 + (y - y_c)^2} \tag{39}$$

III. BOUNDARY CONDITIONS

When the flow is supersonic, the system of differential equations is hyperbolic and boundary conditions must be specified on a U-shaped boundary. Initial conditions specifying uniform flow at the nozzle exit are

$$x = 0: \quad u = \rho = 1, \quad v = S = 0 \tag{40}$$

Along the edges of the free jet the pressure must be atmospheric. This means $p = 1$ or $\rho a^2 = 1$. Using Eq. (29) for the speed of sound,

$$\rho\left[1 + \frac{\gamma-1}{2} M_\infty^2 (1 - u^2 - v^2)\right] = 1 \tag{41}$$

The shape of the jet is not known a priori, but must be determined by applying this boundary condition to the two edge streamlines as the calculations proceed downstream.

IV. NUMERICAL SOLUTION

The three families of characteristics intersect at each of the infinite number of points in the jet. In this section a numerical solution is obtained by using a finite number of points in the jet. To start the numerical solution the width of the jet at the nozzle exit is divided into a number of equally spaced points. The characteristics through these points are found, and the construction of the characteristic mesh is continued downstream in the usual stepwise fashion.

The equation of the characteristics and their corresponding compatibility relations are placed in finite difference from retaining only first order differences for derivatives. The other quantities appearing in the equations are approximated by their average value along the characteristic. The finite difference form of Eqs. (31) - (35) for the typical grid shown in Figure 3 is:

Characteristic I (streamline)

$$v_{34}(x_3 - x_4) - u_{34}(y_3 - y_4) = 0 \tag{42}$$

Compatibility I-a

$$S_3 = S_4 + \frac{\gamma(\gamma-1)M_\infty^2 N(x_3-x_4)}{\rho_{34} a_{34}^2 u_{34}}\left(u_{34}B_{y_{34}} - v_{34}B_{x_{34}}\right)^2 \tag{43}$$

Compatibility I-b

$$\rho_3 = \rho_4 - \frac{N(x_3 - x_4)M_\infty^2}{u_{34}a_{34}^2}\left[u_{34}B_{y_{34}} - v_{34}B_{x_{34}}\right]^2 - \frac{\rho_{34}(S_3 - S_4)}{\gamma}$$

$$\frac{\rho_{34}M_\infty^2}{a_{34}^2}\left[u_{34}(u_3 - u_4) + v_{34}(v_3 - v_4)\right] \qquad (44)$$

Characteristic II

$$(y_3 - y_2)\left[\left(\frac{a_{23}}{M_\infty}\right)^2 - u_{23}^2\right] = (x_3 - x_2)\left[-u_{23}v_{23} - \frac{a_{23}}{M_\infty}\sqrt{u_{23}^2 + v_{23}^2 - \left(\frac{a_{23}}{M_\infty}\right)^2}\right] \qquad (45)$$

Compatibility II-a

$$\left[(u_{23}^2 - v_{23}^2)(x_3 - x_2) + 2u_{23}v_{23}(y_3 - y_2)\right]u_3 + \left[2u_{23}v_{23}(x_3 - x_2) + (v_{23}^2 - u_{23}^2)(y_3 - y_2)\right]v_3 = \left[(u_{23}^2 - v_{23}^2)(x_3 - x_2) + 2u_{23}v_{23}(y_3 - y_2)\right]u_2 + \left[2u_{23}(x_3 - x_2) + (v_{23}^2 - u_{23}^2)(y_3 - y_2)\right]v_2 + \frac{N}{\rho_{23}}\left(u_{23}B_{y_{23}} - v_{23}H_{x_{23}}\right)\left[v_{23}(x_3 - x_2) - u_{23}(y_3 - y_2)\right]\left[B_{y_{23}}(y_3 - y_2) + B_{x_{23}}(x_3 - x_2)\right] - \frac{a_{23}^2(S_3 - S_2)}{\gamma(\gamma-1)M_\infty^2}\left[u_{23}(x_3 - x_2) + v_{23}(y_3 - y_2)\right] - \frac{(\gamma - 1)M_\infty^2 N}{\rho_{23}a_{23}^2}\left[v_{23}(x_3 - x_2) - u_{23}(y_3 - y_2)\right]^2\left(u_{23}B_{y_{23}} - v_{23}B_{x_{23}}\right)^2 \qquad (46)$$

Characteristic III

$$(y_3 - y_1)\left[\left(\frac{a_{13}}{M_\infty}\right)^2 - u_{13}^2\right] = (x_3 - x_1)\left[-u_{13}v_{13} + \frac{a_{13}}{M_\infty}\sqrt{u_{13}^2 + v_{13}^2 - \left(\frac{a_{13}}{M_\infty}\right)^2}\right] \tag{47}$$

Compatibility III-a

$$\begin{aligned}
&\left[(u_{13}^2 - v_{13}^2)(x_3 - x_1) + 2u_{13}v_{13}(y_3 - y_1)\right]u_3 + \left[2u_{13}v_{13}(x_3 - x_1)\right. \\
&\left. + (v_{13}^2 - u_{13}^2)(y_3 - y_1)\right]v_3 = \left[(u_{13}^2 - v_{13}^2)(x_3 - x_1)\right. \\
&\left. + 2u_{13}v_{13}(y_3 - y_1)\right]u_1 + \left[2u_{13}v_{13}(x_3 - x_1) + (v_{13}^2 - u_{13}^2)(y_3 - y_1)\right]v_1 \\
&+ \frac{N}{\rho_{13}}\left(u_{13}B_{y_{13}} - v_{13}H_{x_{13}}\right)\left[v_{13}(x_3 - x_1) - u_{13}(y_3 - y_1)\right]\left[B_{y_{13}}(y_3 - y_1)\right. \\
&\left. + B_{x_{13}}(x_3 - x_1)\right] - \frac{a_{13}^2(S_3 - S_1)}{\gamma(\gamma-1)M_\infty^2}\left[u_{13}(x_3 - x_1) + v_{13}(y_3 - y_1)\right] \\
&- \frac{(\gamma - 1)M_\infty^2 N}{\rho_{13}a_{13}^2}\left[v_{13}(x_3 - x_1) - u_{13}(y_3 - y_1)\right]^2\left(u_{13}B_{y_{13}} - v_{13}H_{x_{13}}\right)^2
\end{aligned} \tag{48}$$

Point 4 in Figure 3 lies on the straight line connecting points 1 and 2 so that

$$\frac{y_1 - y_2}{x_1 - x_2} = \frac{y_4 - y_2}{x_4 - x_2} \tag{49}$$

Assuming that the dependent variables vary linearly from 1 to 2,

$$u_4 = u_2 + (u_1 - u_2)\left(\frac{y_4 - y_2}{y_1 - y_2}\right) \tag{50}$$

$$v_4 = v_2 + (v_1 - v_2)\left(\frac{y_4 - y_2}{y_1 - y_2}\right) \tag{51}$$

$$\rho_4 = \rho_2 + (\rho_1 - \rho_2)\left(\frac{y_4 - y_2}{y_1 - y_2}\right) \tag{52}$$

$$S_4 = S_2 + (S_1 - S_2)\left(\frac{y_4 - y_2}{y_1 - y_2}\right) \tag{53}$$

A single subscript refers to a particular point in Figure 3, while a double subscript indicates an average of the values at the two points.

For the typical grid shown in Figure 3, the location of points 1 and 2 and the values of the dependent variables u, v, ρ, and S at these points is known. Using the twelve Eqs. (42) - (53), the twelve unknowns x_3, y_3, u_3, v_3, ρ_3, S_3, x_4, y_4, u_4, v_4, ρ_4, and S_4 are found. An iteration procedure is used because u_3, v_3, u_4, and v_4 appear non-linearly. For the first iteration, the average value of a quantity which involves point 3 such as u_{i3} is approximated by u_i.

The first quantities to be computed are the coordinates x_3, y_3 of the intersection of the II and III characteristics. These are obtained by simultaneous solution of Eqs. (45) and (47). Similarly, the intersection x_4, y_4 of the streamline characteristic with the straight line connecting points 1 and 2 is found from Eqs. (42) and (49). The values of u_4, v_4, ρ_4, and S_4 can then be found from

Eqs. (50) - (53). The compatibility equations (43) and (44) yield values for S_3 and ρ_3, respectively. u_3 and v_3 are obtained by simultaneous solution of Eqs. (46) and (48). This completes the first iteration. These calculations are repeated until the numerical values of the dependent variables converge to the desired degree of accuracy.

All points in the interior of the jet are solved in the manner described above. Points on the upper and lower edges of the jet must be treated in a different manner since only two families of characteristics intersect. A typical mesh on the lower boundary of the jet is shown in Figure 4. The location of points 1 and 4 and the values of dependent variables at these points are known. The six unknowns, x_3, y_3, u_3, v_3, ρ_3 and S_3, are found from Eqs. (42), (43), (44), (47), (48) and the condition

$$p_3 = 1 \tag{54}$$

which states that the pressure along the edge streamlines of the jet must be atmospheric. A more useful form of this equation is

$$\rho_3\left[1 + \frac{\gamma-1}{2} M_\infty^2(1 - u_3^2 - v_3^2)\right] = 1 \tag{55}$$

The calculations for a boundary point begin with the simultaneous solution of Eqs. (42) and (47) for x_3 and y_3. Next, S_3 is obtained from Eq. (43), and ρ_3 from Eq. (44). Then u_3 and v_3 are found by simultaneous solution of Eqs. (48) and (55). This completes one iteration.

The iteration procedure described above did not converge when average values between points 1 and 3, and points 4 and 3 were used for u, v, and ρ. In order to make the iteration procedure converge, we introduce the weighting factors α, β, and ζ so that

$$u_{i3} = \tfrac{1}{2}[u_i + \alpha u_3] \tag{56}$$

$$v_{i3} = \tfrac{1}{2}[v_i + \beta v_3] \tag{57}$$

$$\rho_{i3} = \tfrac{1}{2}[\rho_i + \zeta \rho_3] \tag{58}$$

The subscript i is 1 or 4 for the lower boundary of the jet and is 2 or 4 for the upper boundary. These equations reduce to those for average values when $\alpha = \beta = \zeta = 1$. For the examples treated in the report, rapid convergence was obtained with $\alpha = 0.4$, $\beta = 0.9$, and $\zeta = 0.7$.

The last quantity to be computed is the reaction force at the wire. This is obtained by summing the components of the equal and opposite body force acting on each diamond-shaped mesh. For the typical mesh shown in Figure 5, the area is

$$A = \sqrt{s(s-a)(s-b)(s-c)} + \sqrt{s'(s'-c)(s'-d)(s'-e)} \tag{59}$$

where

$$\begin{aligned} s &= \tfrac{1}{2}(a + b + c) \\ s' &= \tfrac{1}{2}(c + d + e) \end{aligned} \tag{60}$$

Using Eqs. (36) and (37), the components of the body force acting over the area A are approximated by

$$F_x = N\left\{\left[uB_y - vB_x\right] B_y\right\}_{avg} A \tag{61}$$

$$F_y = -N\left\{\left[uB_y - vB_x\right] B_x\right\}_{avg} A \tag{62}$$

where

$$\{\ \}_{avg} = \tfrac{1}{4} \sum_{i=1}^{4} \{\ \}_i \tag{63}$$

V. RESULTS AND CONCLUSIONS

The first case to be considered is shown in Figure 6. The jet leaves the nozzle exit with $M_\infty = 2.0$ and interacts with the magnetic field produced by a wire located at (0,3). Calculations were made for the interaction parameter $N = 0.1$. The interaction bends the jet upward and decelerates the flow. At $X = 10$, the upper edge of the jet has been displaced twice as much as the lower edge so that the width of the jet has doubled. Contour lines of constant Mach number and u appear in Figures 7 and 8, respectively. Since the flow is rotational, the entropy increases along streamlines as indicated by Figure 9. The density decreases in the streamwise direction even though the velocity is also decreasing. Contour lines of constant density are plotted in Figure 10.

In Figure 11 the components F_x and $-F_y$ of the reaction force at the wire are plotted for two locations of the wire, the solid curves for (0,3) and the dashed curves for (0,1.5). For the range of N considered the components vary linearly with N except near $N = 0$. The magnitude of the reaction force increases directly with N and its inclination is fixed in the downstream direction toward the jet. Thus, the jet tends to drag the wire with it. Care must be taken in comparing the two sets of curves for the same value of N, for N is proportional to B_o, the value of the field at the origin. To keep B_o fixed, the wire at $y_c = 3$ must carry twice the current of the wire at $y_c = 1.5$. Although at $y_c = 1.5$ the wire is closer to the jet near the exit, the downstream portion of the jet

is about equidistant from both locations due to the bending of the jet. These factors, along with the greater area downstream for interaction, leads to the greater force on the wire at the outer location $y_c = 3.0$.

The next two figures show the jet when the wire is located at (20,3) which is far downstream of the nozzle exit at x = 0. In Figure 12 $M_\infty = 4.0$ and N = 0.1. The jet slows down and reaches the sonic velocity near x = 16. The two edge streamlines are almost symmetric and bend so that the width of the jet at x = 16 is 2.5 times the exit width. It is interesting to note the smooth deceleration without the appearance of shocks as in the case of the channel flow considered in Reference 3.

In Figure 13 $M_\infty = 2.0$ and N = 0.05. The interaction is weak enough to permit the jet to pass the wire at x = 20. Along the upper streamline at x = 27 the Mach number has reached unity. The upper streamline has been displaced very little, while the lower streamline has moved downward to increase the width of the jet by a factor of two. The components of body force are $F_x = 0.22$ and $F_y = -0.012$.

REFERENCES

1. Hains, F.D. and Ehlers, F.E., "Interaction of a Plasma Jet with a Magnetic Field", Proceedings of 1962 Heat Transfer and Fluid Mechanics Institute, Stanford University Press, Stanford, California, 1962.

2. Joos, Georg, Theoretical Physics, 2nd Edition, Blackie and Son, Ltd., London, 1951. pp 108-109.

3. Hains, F.D., Yoler, Y.A., "Axisymmetric Magnetohydrodynamic Channel Flow", Journal of the Aerospace Sciences, Vol. 29, No. 2, pp. 143-150, February 1962.

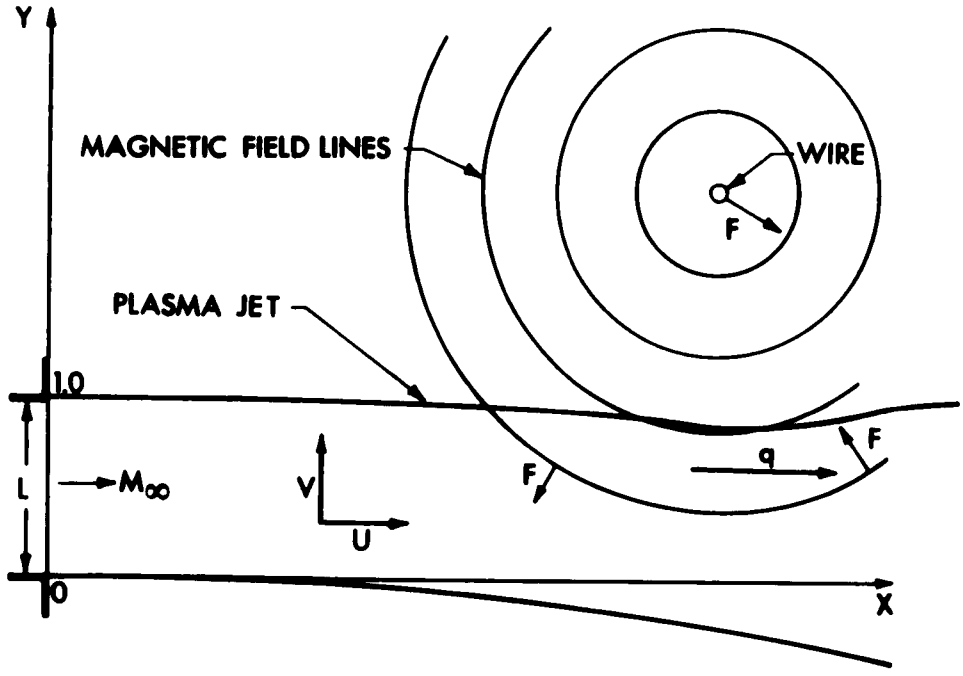

Figure 1. INTERACTION OF A PLANE JET WITH A MAGNETIC FIELD. WIRE LOCATED DOWNSTREAM OF THE JET EXIT.

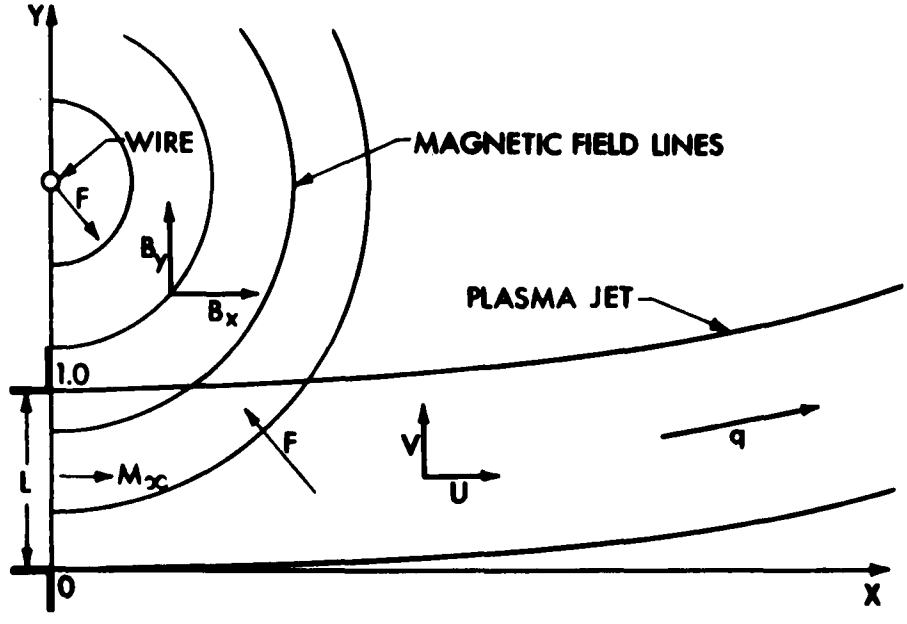

Figure 2. INTERACTION OF A PLANE JET WITH A MAGNETIC FIELD. WIRE LOCATED IN EXIT PLANE OF JET.

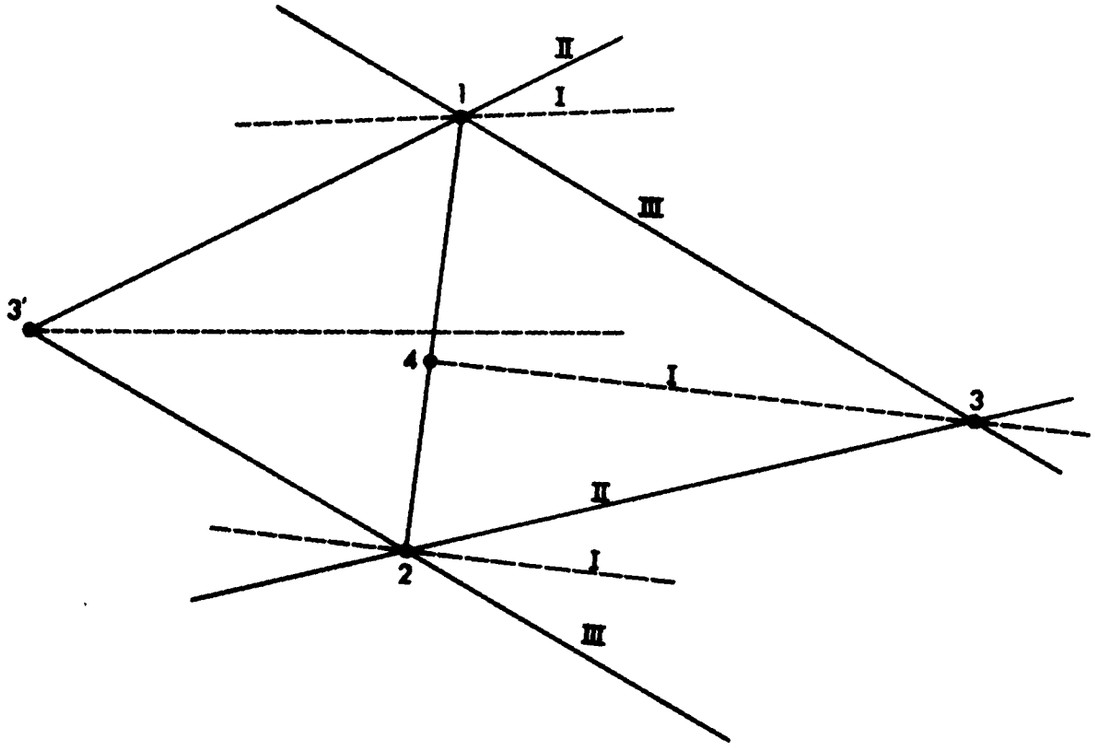

Figure 3. TYPICAL CHARACTERISTIC GRID FOR INTERIOR OF JET.

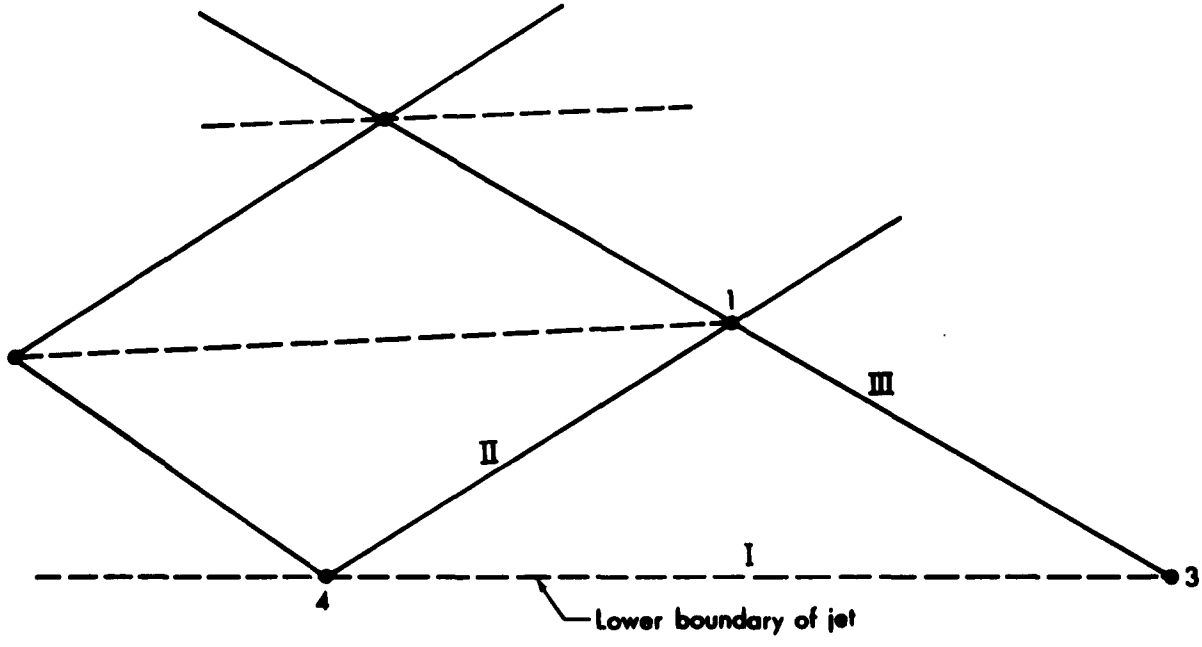

Figure 4. TYPICAL CHARACTERISTIC GRID ALONG LOWER BOUNDARY OF JET.

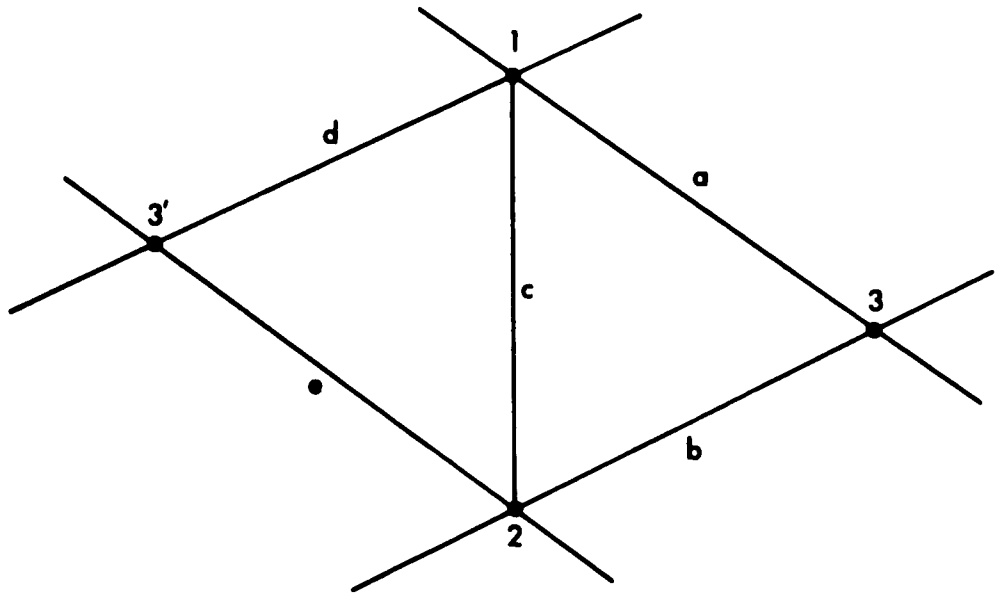

Figure 5. TYPICAL CHARACTERISTIC GRID WHOSE AREA IS GIVEN BY EQ. (59).

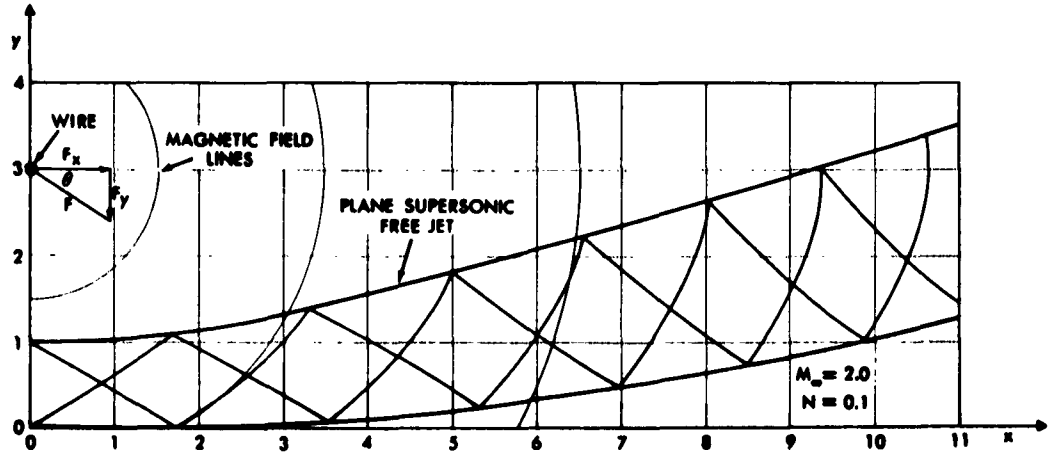

Figure 6. JET SHAPE AND CHARACTERISTICS FOR M_∞ = 2.0 AND N = 0.1

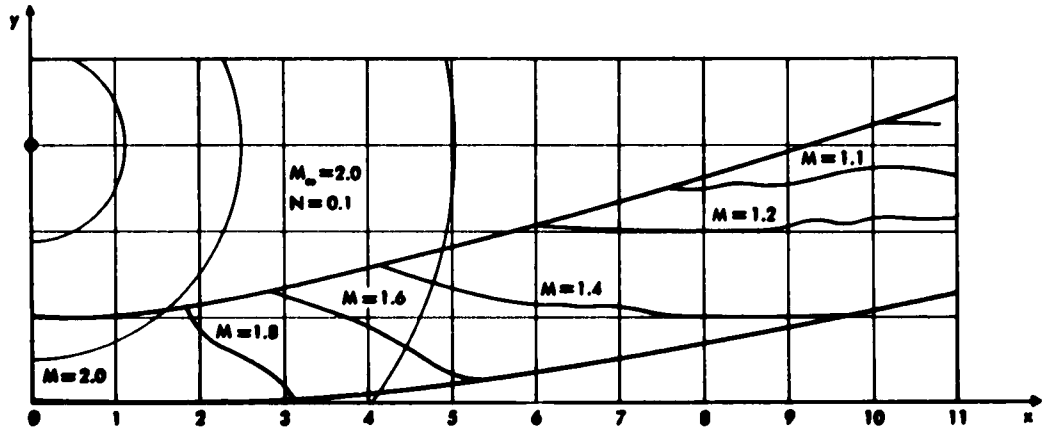

Figure 7. CONTOUR LINES OF CONSTANT MACH NUMBER.

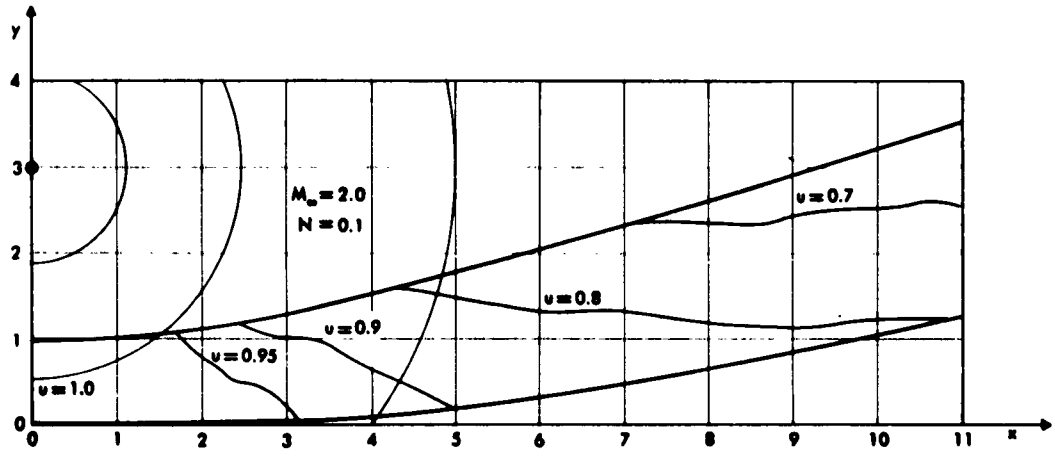

Figure 8. CONTOUR LINES OF CONSTANT u.

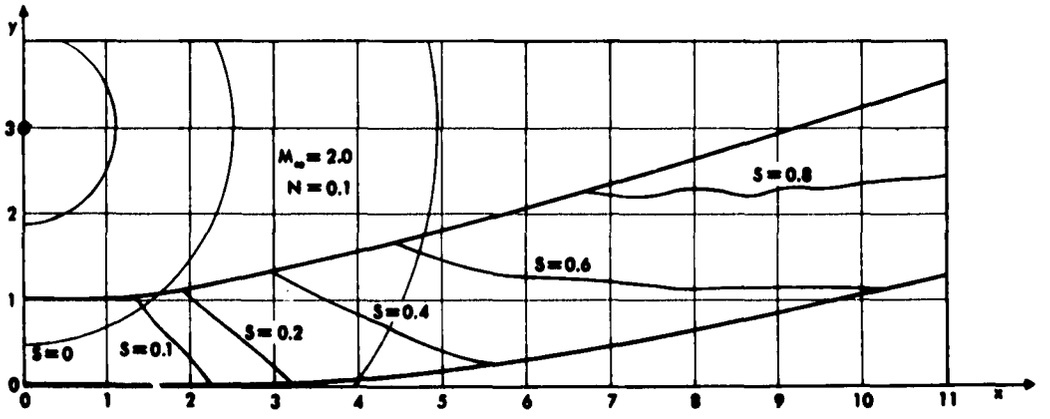

Figure 9. CONTOUR LINES OF CONSTANT s.

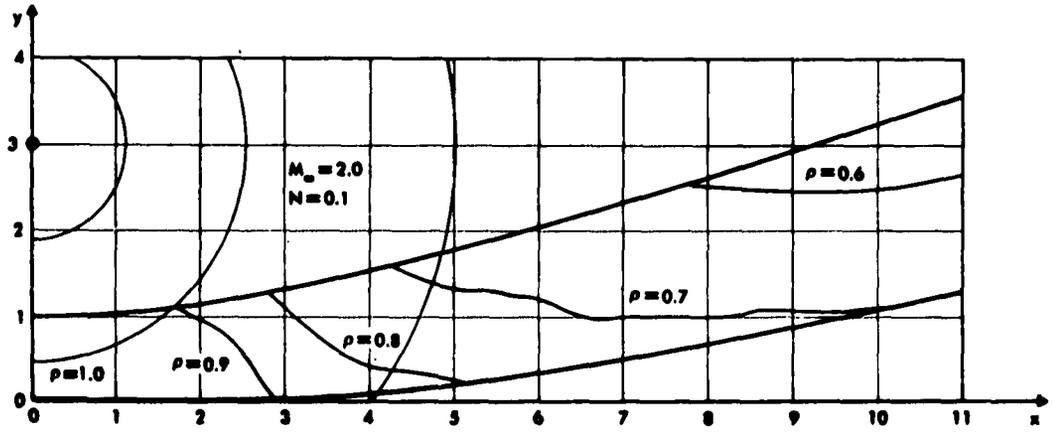

Figure 10. CONTOUR LINES OF CONSTANT ρ.

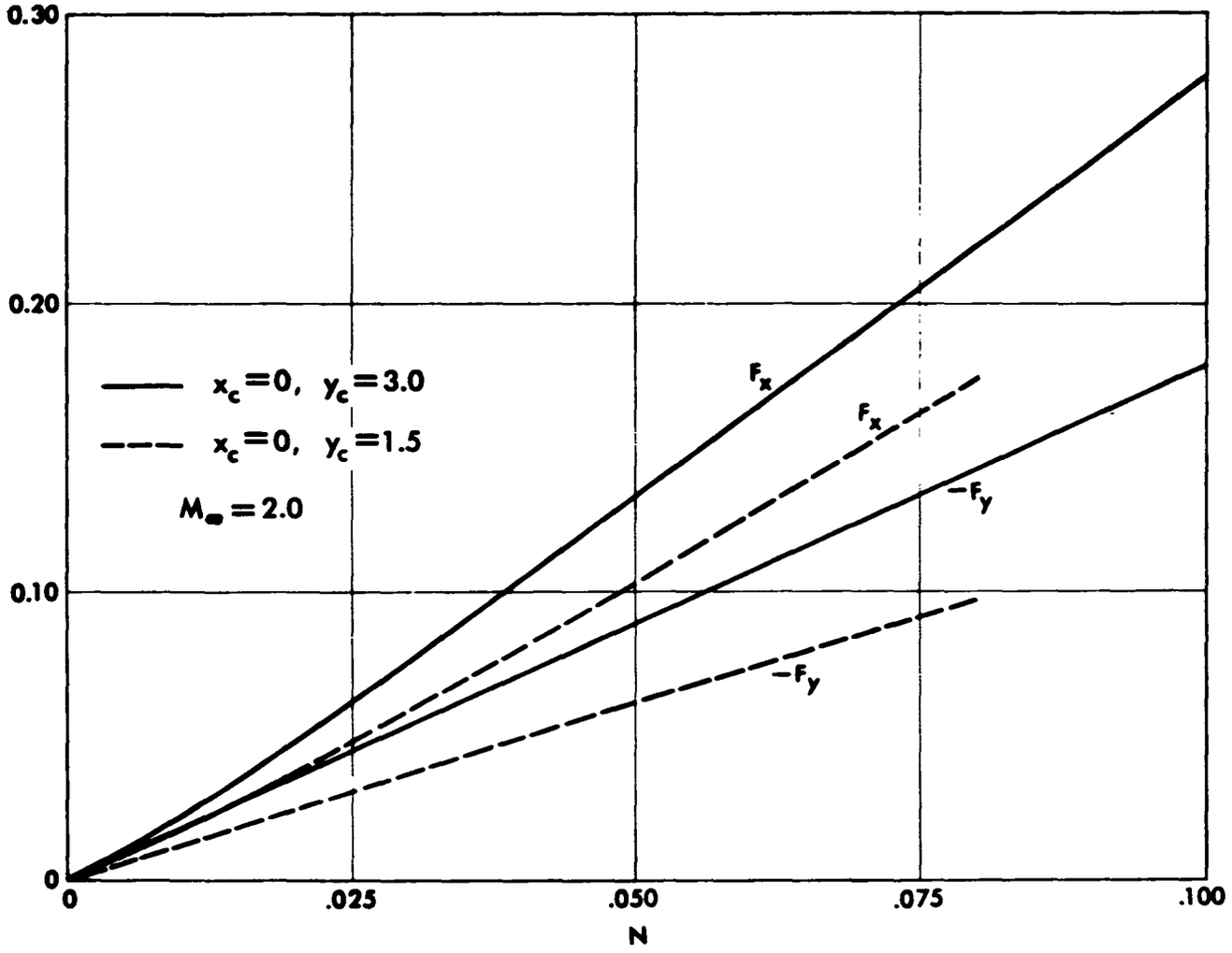

Figure 11. REACTION FORCE AT THE WIRE vs N

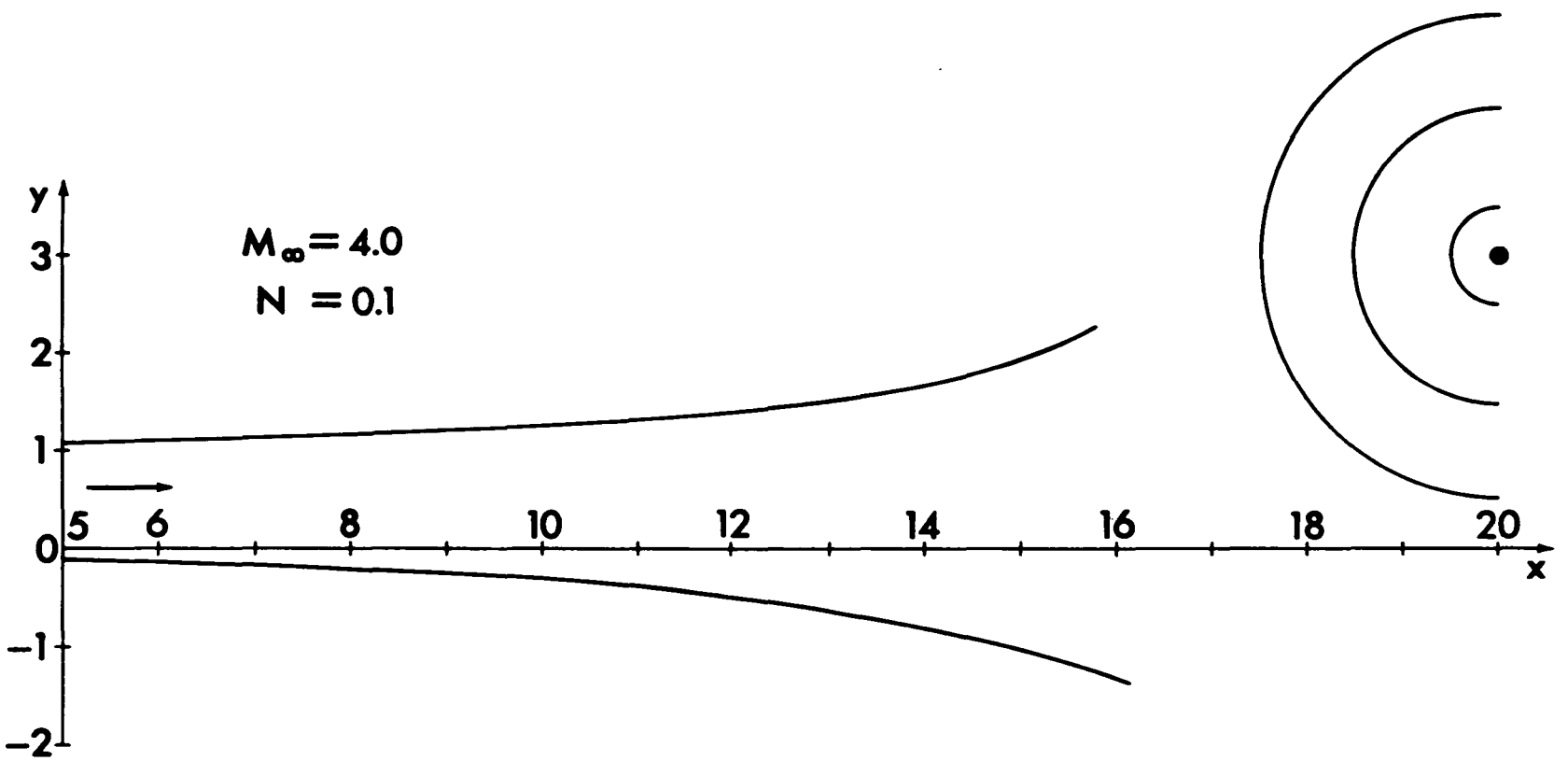

Figure 12. JET SHAPE FOR M_∞ = 4.0 AND N = 0.1

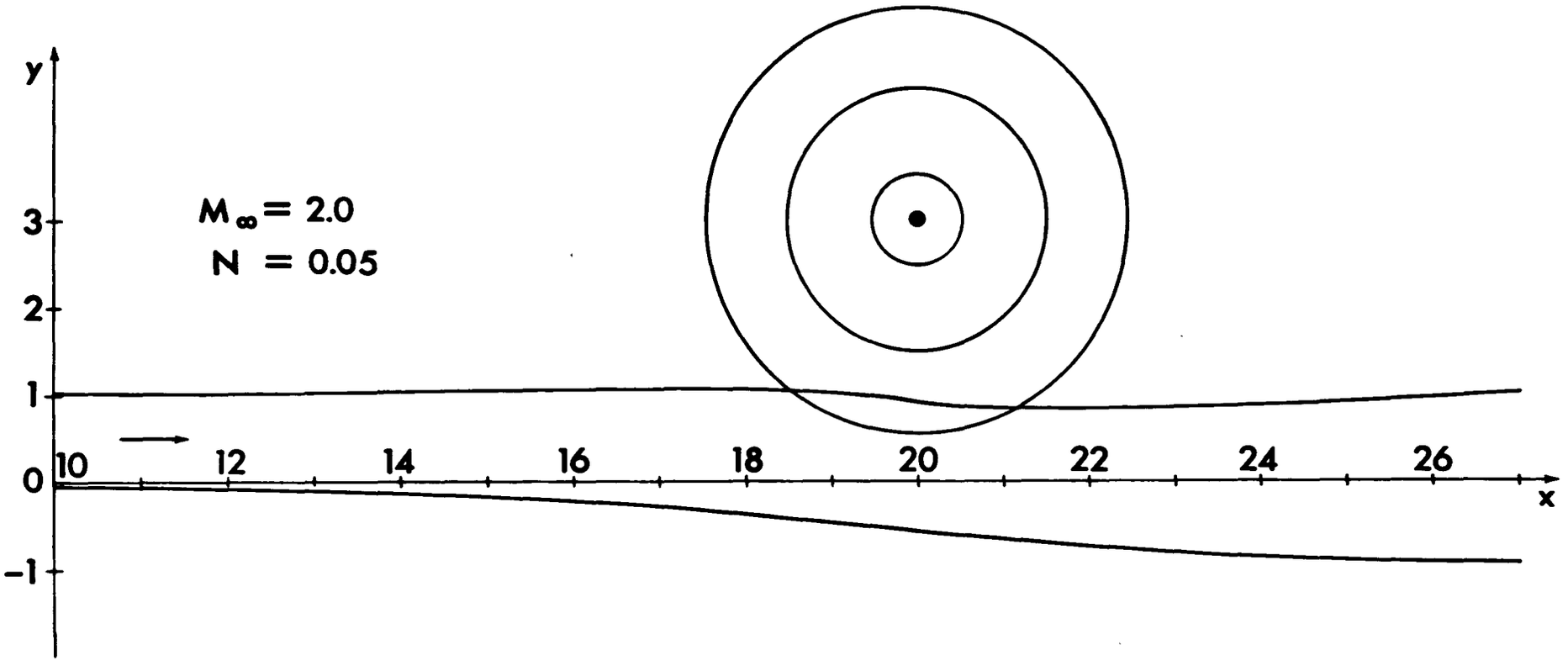

Figure 13. JET SHAPE FOR M_∞ = 2.0 AND N = 0.05